Models of Development

Anders Sandberg

January 21, 2003

Abstract

The central question of development is: how does structure emerge from a structureless state without an external organizing force? The answer seems to be that self-organizing processes are able to produce complex structures from simple initial states. In biological systems a major factor appears to be diffusion of chemical factors guiding growth or differentiation. The interaction between different diffusible factors can create pattern forming instabilities giving rise to differentiation of initially homogeneous tissue. By following gradients axons can connect with the right target cells, setting up neural networks. This paper is a review of models of biological pattern formation and development.

1 Introduction

In the brain there are $\approx 10^{11}$ neurons with $\approx 10^4$ synapses each, but the number of human genes are likely on the order of a few tens of thousand [1] – a large number, but far too few to specify the exact connectivity or position of the neurons even if they can express many more proteins.

Self organization allows random or similar units to produce organized and possibly very complex patterns without the need for a complex "recipe". It works by symmetry breaking: the initial undifferentiated state is an unstable equilibrium where deviations are amplified by positive feedback. Random noise in the initial state acts as a seed for the pattern, which can be highly regular and reliable despite the random origin.

A simple recipe for a complex brain:

1. Grow a large number of similar cells.

2. Allow them to differentiate into different types of neurons depending on their local chemical environment.

3. Diffuse long-range chemical signals.

4. Let different types of neurons send out connections towards their preferred chemical.

5. Connect, and possibly remove failed cells and connections.

This can be iterated, and influenced by neural activity and experience from the outside.

This is a special case of development, combining both local cellular processes where individual neurons develop their shapes, patterning on both local and global scales, and the development of structures in response to these patterns.

In the following I will review some models of development and morphogenesis, the creation of bodies and form.

2 Reaction-Diffusion Systems

2.1 Turing patterns

In 1952 Alan Turing published a paper [2] showing how patterns might grow from a nearly homogeneous situation and how diffusion could drive an instability. (In the following, I am borrowing the description from [3])

Turing considered a one-dimensional chain of identical cells ($k = 1, 2, \ldots N$) containing various chemicals he called *morphogens* (form producers). If there are m morphogens, the internal dynamics of each cell is controlled by m coupled linear differential equations, while the coupling between the cells is modeled by a simple diffusion process through the cellular membrane. It is not a real biochemical model but rather a simple linearization of one.

A simple example with two morphogens with concentrations X_k and Y_k. Consider small deviations from the equilibrium state so that $X_k = X^0 + x_k$ and $Y_k = Y^0 + y_k$. Then Turing's linear model is described by the equations

$$x'_k = ax_k + by_k + \mu[(x_{k+1} - x_k) - (x_k - x_{k-1})] \tag{1}$$

$$y'_k = cx_k + dy_k + \nu[(y_{k+1} - y_k) - (y_k - y_{k-1})] \tag{2}$$

where μ and ν are diffusion coefficients for the morphogens x and y respectively. The coefficients a, b, c and d are constant and assumed to be set so that isolated cells have a stable dynamics: $a + d \leq 0$ and $ad - bc > 0$. If these inequalities hold $x, y \to 0$ over time.

It should be noted that these conditions force the signs of the matrix

$$\begin{pmatrix} a & b \\ c & d \end{pmatrix} \tag{3}$$

into the forms

$$\begin{pmatrix} + & + \\ - & - \end{pmatrix} \begin{pmatrix} - & - \\ + & + \end{pmatrix} \begin{pmatrix} + & - \\ + & - \end{pmatrix} \begin{pmatrix} - & + \\ - & + \end{pmatrix} \tag{4}$$

The first two alternatives corresponds to a self-amplifying activator and a depleted substrate. The second two alternatives corresponds to an activating substance and an inhibiting substance where the activator activates itself and the other, while the second substance inhibits itself and the first. See [4] for a
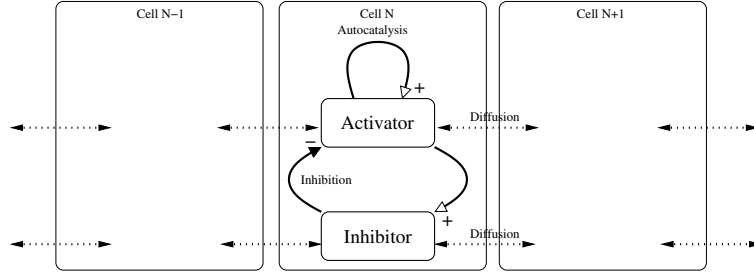
Figure 1: Activator-inhibitor system in a linear chain of cells. The activator stimulates production of more activator and inhibitor, while the inhibitor decreases activator production. Both chemicals diffuse between cells.

more detailed analysis. For three-component systems the distinction between activator and inhibitor/substrate becomes unclear.

We are used to that diffusion always smoothes out spatial inhomogeneities. Turing showed that in this case nonzero μ and ν can lead to the emergence of growing patterns – small disturbances will become large spatial patterns. The reason our intuition doesn't work here is that normally diffusion is about diffusing scalar quantities, but in this case we actually have a diffusion of a vector quantity, the pair (x, y).

Assume periodic boundary conditions so that $x_k(t) = x_{k+N}(t)$ and $y_k(t) = y_{k+N}(t)$ (a ring of cells).

Introduce normal modes with amplitudes $(\xi_s(t), \eta_s(t))$ (i.e. we look at how different Fourier components change over time):

$$(x_k, y_k) = \sum_{s=0}^{N-1} (\xi_s, \eta_s) \exp(2\pi i k s/N) \tag{5}$$

which satisfy the boundary conditions and an orthogonality relation

$$\sum_{k=1}^{N} \exp(2\pi i k(s - s')/N) = \begin{cases} N & \text{if } s - s' = 0, N \\ 0 & \text{otherwise} \end{cases} \tag{6}$$

Using equation 2–6 we get the dynamic equations for the normal modes:

$$\xi_s' = (a - 4\mu \sin^2(\pi s/N))\xi_s + b\eta_s \tag{7}$$

$$\eta_s' = c\eta_s + (d - 4\nu \sin^2(\pi s/N))\eta_s \tag{8}$$

These equations are decoupled for different values of s (different Fourier modes do not interact) and are hence easier to analyze.

If we introduce $\sigma = \sin^2(\pi s/N)$ ($1 \geq \sigma \geq 0$) and

$$a_\sigma = a - 4\mu\sigma \tag{9}$$

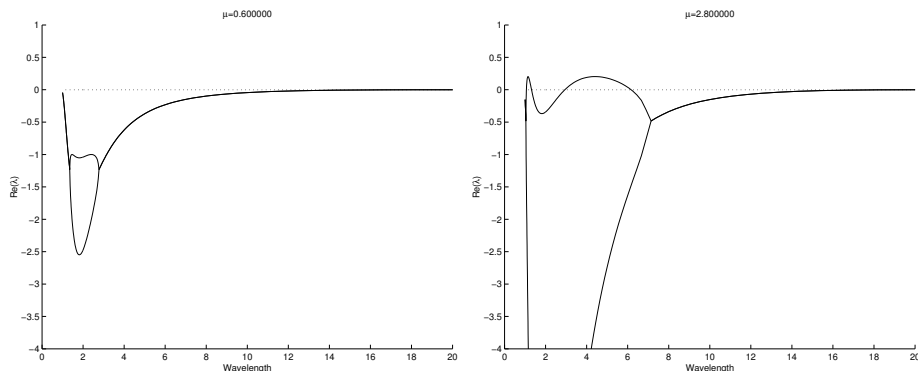$$d_\sigma = d - 4\nu\sigma \tag{10}$$

Figure 2: Stability of different wavelength modes for different values of the diffusion parameter μ. The real parts of the characteristic exponents of different modes of a 20 cell chain with the coefficients $\nu = 0.3, a = -1, b = 1, c = -2, d = 1$ are plotted as a function of their wavelength. To the left $\mu = 0.6$, all exponents are negative and disturbances decay regardless of their wavelength. The "bubble" is caused by the existence of two exponents. To the right $\mu = 2.8$, some modes have become unstable (a $\lambda > 0$) and hence will grow rapidly. This corresponds to the formation of regular patterns with wavelength 4.

the characteristic exponents ($\xi, \eta \propto \exp(\lambda t)$) become

$$\lambda = \frac{1}{2}(a_\sigma + d_\sigma) \pm \frac{1}{2}\sqrt{(a_\sigma + d_\sigma)^2 + 4(bc - a_\sigma d_\sigma)} \qquad (11)$$

When the real part of an exponent becomes positive that mode will become unstable, and any deviation from $\xi = \eta = 0$ will grow over time. This means that (x_k, y_k) will start to behave like a growing sinus-curve and no longer remain spatially homogeneous.

For the case $\mu = \nu = 0$ the system starts in the region where the two eigenvalues have negative real parts, and $\xi_s, \eta_s \to 0$. As μ and ν are increased above zero they will in the general case make λ gain a positive real part for one or more s, ξ_s and η_s will not be attracted to 0, and small disturbances will instead grow exponentially. A plot of λ as a function of wavelength can be seen in figure 2.

Modes with smaller exponents will not grow as fast as the one with the largest exponent, and hence it will dominate the pattern after a while.

An important relation is that $\mu \neq \nu$; if they are equal the instability cannot develop. This is a problem when applying this kind of model to systems in solution, as the diffusion coefficients of many chemicals are of the same order of magnitude. However, the ratio μ/ν can become very close to 1 and the system still exhibit instability if the Hill coefficients are high enough [4]. Turing pattern formation is notably easier to produce experimentally in a solid + solution situation.

This model is fairly crude, the concentrations of morphogens grow without bound and are not related by any biochemical kinetic equations. A more realistic model would introduce a nonlinearity keeping the concentrations bounded. For example, Turing developed an example system

$$X'_k = \frac{1}{32}(-7X_k^2 - 50X_kY_k + 57) + \mu(X_{k+1} - 2X_k + X_{k-1}) \qquad (12)$$

$$Y'_k = \frac{1}{32}(7X_k^2 + 50X_kY_k - 2Y_k - 55) + \nu(Y_{k+1} - 2Y_k + Y_{k-1}) \qquad (13)$$

with $\mu = 1/2$ and $\nu = 1/4$. Using the University of Manchester computer he solved this in 1951 for a 20 cell ring, and found stable patterns.

The general reaction-diffusion system is written as

$$\boldsymbol{x}' = \boldsymbol{f}(\boldsymbol{x}) + \boldsymbol{D}\nabla^2\boldsymbol{x} \qquad (14)$$

where $\boldsymbol{D}$ is a diagonal matrix of diffusion coefficients and $\boldsymbol{f}$ the reaction interaction. Although the equation has no preference for any special symmetry, it is common for systems like this to exhibit complex symmetry breaking patterning.

An important example is the complex Ginzburg-Landau equation ($\boldsymbol{f} = az - b|z|^2z$, where a, b and z are complex numbers), which appears in physical models of super-conductivity, super-fluidity and nonlinear waves. The real and imaginary components of z act as activator and inhibitor, and enables a wide variety of possible patterns in one, two and three dimensions [5]. The reaction-diffusion pathway to pattern formation is very general. It can even describe "the wave" in the crowd of a football stadium [6].

2.2   1D Reaction-Diffusion Systems

Hans Meinhardt has studied the development of the Hydra [7, 8]. The animal has a foot, a body and a head with tentacles. If the body is split in two both halves develop into full hydras. He models this by having an activator-inhibitor pair with a diffusion length comparable to the body. As the body becomes longer the homogeneous state becomes unstable and a single maximum occurs at one end of the body, where the head develops. If the body is cut, the concentration gradients adjust (more quickly in the head piece) and results into two similar gradients with the same orientation. Other morphogens linked to the main gradient can be introduced to explain foot and tentacle differentiation.

Segmentation can be explained [7, 8] using morphogen-regulated genetic expression. From a default gene state different genes become progressively activated by higher morphogen concentrations, forming a sequence along a morphogen gradient.

Shugo Hamahashi and Hiroaki Kitano have studied the embryogenesis of Drosophila melanogaster [9]. The model is based on reaction-diffusion system where a number of gene transcription products diffuse within the cyncytium of the fly egg.

The pattern formation is regulated by the maternal genes (genes with inhomogeneous distribution of mRNA at egg-laying), which regulate the polarity of

the fly. These genes in turn control the gap genes which determine body segmentation and in turn regulate pair-rule genes that determine segment polarity and hometoic genes (which determine the developmental fate of each segment).

The model consists of diffusion of proteins along the body, with protein production determined by transcription which occurs if promoting proteins have concentrations within a certain range. Parameters are tuned using a genetic algorithm [10]. The resulting patterns fit well with known patterning, and can replicate many of the effects of mutations in the developmental system.

Meinhardt has modeled the patterns on sea shells using 1D diffusion-reaction systems [11]. As the snail grows, material is added at the growing edge and this is where pigments are inserted by pigment producing cells. Parallel lines are produced by spatially static patterns of pigmentation, while perpendicular lines are produced by synchronous oscillations along the growing edge and oblique patterns can be produced by traveling waves. With several morphogens it is possible to produce a wide variety of patterns found on sea shells.

2.3 2D Reaction-Diffusion Systems

A nice demonstration of the variety of patterns and dynamic behaviors that can occur in a two-morphogen system in two dimensions is the Xmorphia website [12] which explores the patterns found in the system

$$U' = -UV^2 + F(1 - U) + D_U \nabla^2 U \tag{15}$$

$$V' = UV^2 - (F + k)V + D_V \nabla^2 V \tag{16}$$

where $D_U = 2 \cdot 10^{-5}$, $D_V = 10^{-4}$ for different values of F and k.

In general, reaction-diffusion models of this kind can produce stripe patterns, labyrinths, spots and spirals, both stationary and non-stationary [5]. This has been taken as a model for fur texture, fish patterning [13], butterfly wing patterns and limb disc formation [7, 14].

In 2D the extra dimension allows further symmetry breaking. Since the reaction-diffusion equations do not contain any preference for any particular direction different unstable modes with the same spatial frequency but different directions will compete with each other. Often the result is a regular square or hexagonal pattern, although the order is often just local. If the morphogens diffuse with different speeds in different directions the pattern tend to align with a certain direction [15].

Striped patterns are in general less easy to generate than spotted patternss. In two reactant reaction-diffusion systems stripe patterns tend to dissolve into spots; by adding further reactants or changing the nonlinearity they can be stabilized [16].

As a rule reaction-diffusion patterns are influenced by the shape of the domain where diffusion takes place. This can cause the change from spot-like patterns to stripes when the domain is narrowed (as in the leopard's tail), boundary effects and on closed domains such as circles or spheres geometric restrictions on patterns can induce symmetries [17]. When two reaction-diffusion systems

producing stripes meet, for example where a limb of a striped animal meets its body, a chevron pattern emerges which fits well with the patterning of the Zebra [18].

The size of elements of the pattern are set by the diffusion coefficients. If the underlying substrate of the pattern (such as the skin of an animal or the edge of a mollusk shell) is growing features of the pattern (such as spots or stripes) will retain their size but more features will appear as more space appears. For example, the angelfish develops more strips as it grows [19], which is evidence that its patterning is regulated by an ongoing process. In a similar manner growing conical shells can exhibit increasing number of stripes [11]. Other animals lay down their patterning during early development when their bodies are smaller, and as they grow they retain the fixed pattern. This produces fewer spots or stripes than if they emerged on later stages, and animals with smaller embryos and shorter gestation periods tend to have simpler patterns [20, 21, 16]

3 Neurite Formation

During early development neurons start out rounded, but develop protrusions of the cell membrane which later grow into neurites. The neurite with the highest outgrowth rate often becomes the axon while the others become dendrites [22].

The branching shape of neurons may be due to activity-dependent effects deforming the cell membrane. Especially the amount of calcium, increased by electric activity, and neurotrophic factors secreted by other cells or growing dendrites appear to be important.

One such model of activity dependent dendritic morphogenesis has been created by Hentschel and Fine [23]. They model the growth of isolated initially spherical cells, where outgrowth and retraction of the cell membrane are taken to depend upon the local concentration of Ca^{2+} on the inside:

$$V(s) = a[Ca^{2+}] - b[Ca^{2+}]^2 \tag{17}$$

where $V(s)$ is the growth normal to the surface at point s and a and b constants. The calcium ions diffuse within the cell and are affected by membrane ion pumps. As the concentration increases the local membrane potential is changed and voltage-gated calcium channels may open, further increasing the concentration.

At a slightly convex patch of membrane more calcium will diffuse into the local volume than at a flat or concave patch, resulting in a positive feedback loop causing local membrane growth. As the membrane grows, more surface will surround the volume and the calcium level will increase faster. At first the elongation caused by this growth is straight, but eventually it becomes unstable and branches, producing dendrite-like structures.

Another model is due to Hely, van Ooyen and Willshaw [24, 25]. They model the behavior of a growth cone as a reaction-diffusion system with calcium as an activator and cAMP as inhibitor. Calcium drives filopodia outgrowth, with retraction if the concentration is too high. Simulations for a 10μm growth cone shows a hot spot of high calcium concentration emerging at one side, causing

the localized extensions of filopodia. This model could also be regarded as a model of neurite formation, and appears quite compatible with the Hentschel and Fine model.

See also [22] for a review on other forms of activity-dependent neural network development.

4 Dendrites

Hely, Graham and van Ooyen has developed a model of dendrite elongation and branching based on the interaction of calcium and MAP2 [26, 25]. MAP2 binds to microtubuli in the dendrites and stabilize them. As it is phosphorylated it moves the microtubuli further apart, making branching more likely.

Neurons are modeled as compartments containing calcium and MAP2 (which in turn can be unbound, bound and phosphorylated). The chemical concentrations are modeled using coupled differential equations, describing the diffusion of MAP2 out from the soma, calcium influx and various reaction pathways binding MAP2 to microtubuli. The start situation has a spherical cell with a single dendritic compartment. The simulation is run with a time-step dt, during which the terminal compartments are elongated by dx until they reach length $2dx$, when they are split transversally into two dx compartments, one of which is terminal. At each time-step the terminal compartment may split into two branches with a probability P_{branch} dependent on the local concentration of bound and phosphorylated MAP2.

The model can produce dendritic trees with branching patterns similar to biological neurons, with properties such as decreasing probability of branching, similar levels of asymmetry, length and degree.

5 Axonogenesis

During development of the nervous system neurons send out axons which migrate towards their targets. One of the mechanisms guiding the axons is the diffusion of chemoattractant molecules such as netrins and neurotrophins through the extracellular space. These molecules create a gradient of increasing concentration which can be sensed and followed by the growth cone of the growing axon[1]. There also exists chemorepellants which turn the axons away from certain tissues.

Contact adhesion and repulsion with the substrate (other cells and the extracellular matrix) also mediate short range decisions of growth through receptors in the growth cone. Growing axons can also lay down labelled pathways, that other axons can follow. This is mediated by N-CAM, cadherins and fasciclins. However, the pioneer axon must use chemotaxis to find its way.

---

[1]This was originally suggested by Ramon Y Cajal in 1893.

5.1 Guidance

One important issue is how far chemical gradients can guide axons. At one end of the growth cone the concentration of the chemoattractant is C, at the other $C + \Delta C$. In order to move towards the gradient the cone needs to detect and measure the difference. This is done by averaging, over some time period, the number of bound receptors at one end compared to the other.

This introduces some physical limitations [27]. If the concentration is low compared to the dissociation constant of the receptor then few receptors will be bound and guidance become hard. If the concentration is so high that most receptors are bound, then there is also too little information to guide the growth. Finally, the difference ΔC across the growth cone must be large enough to overcome the noise in the binding process and in the intracellular signalling that turns a binding difference into directional information.

A simple model (described in [27]) giving an estimate of the sensitivity assumes a concentration $C = q/(4\pi D r)$, where D is a diffusion coefficient (for netrin-1 in collagen 10^{-7} cm^2 s^{-1}), q a production rate ($\approx 10^{-7}$ nM/s) and r the distance.

The minimal concentration change that can be detected is around 1%. If the growth cone with width Δr detects the fractional change $\Delta C/C$, then we get

$$\frac{\partial C}{\partial r} \frac{\Delta r}{C} \geq 0.01 \tag{18}$$

which produces a maximum guidance distance $r_{max} = 100\Delta r$. For a 10μ growth cone $r_{max} = 1$ mm.

If the growth cone detects absolute changes

$$\frac{\partial C}{\partial r} \Delta r \geq \frac{K_D}{100} \tag{19}$$

$$r_{max} = 5\sqrt{\frac{q\Delta r}{\pi D K_D}} \tag{20}$$

which also, coincidentally, for likely values of the constants produces $r_{max} = 1$ mm.

Goodhill also shows that this range can be extended to ≈ 1 cm by providing a optimally shaped gradient of chemoattractant bound to the substrate. The range can also be extended by exploiting receptors further away on the axon (increasing Δr). In nature, many other forms of chemotaxis are common, and models suggest that there exists many trade-offs between different parameters in order to optimize the growth or movement [28].

5.2 Bundling

Hentschel and van Ooyen describe a model of axon guidance and bundling [29]. Axons originate at a cluster of cells and are attracted towards another cell cluster. The model includes three kinds of diffusible molecules:

9

- A chemoattractant that is released by the target cells. This serves to guide the axons towards their targets.

- A chemoattractant that is released by the axon growth cones. This makes the axons bundle together.

- A chemorepellant that is released by the axon growth cones at a rate dependent on the concentration of target chemoattractant. This serves to dissolve the bundle on reaching the target area.

The chemicals are modeled as diffusive fields with point sources in the cells or cones, and different diffusion constants and rates of production. It is assumed that the speed of diffusion is larger than the speed of cone growth. The growth cones will grow along the weighted sum of the local concentration gradients.

This model is able to demonstrate fasciculation, axon guidance and defasciculation and target innervation. It was found that target derived chemoattractant gradients were not enough to debundle the axons, the chemorepellant was necessary. The organization of innervation is not random but topologically ordered due to the organization in the initial bundling.

A second model of the authors deals with contact interactions between the growth cones instead of diffusion. Bundling occurs when two axons grow close together and has a strength dependent on the concentration of target chemoattractant.

It was found that only local bundling occurs, with no tendency for global bundling. Some axons grow towards the targets at a faster rate, creating paths for others to follow. Debundling does not occur well.

6 Cellular Approaches to Development Modeling

Reaction-diffusion models generally assume a continuous field or a regular array of identical cells, and the dendrite and axon models discussed above mainly deal with a single cell. More complex simulations deal with cells that can be arranged arbitrarily, move or divide.

The perfect C. elegans project [30] attempts to model all the cells in C. elegans and to fill in missing data with simulated cells. The model computes forces between cells using inverse kinematics.

Kurt Fleischer has developed a multicellular developmental model for simplified cells including effects of diffusion of chemical signals, cell collisions, adhesion, cell recognition and motion equations. Cells are spheres able to move, divide, release diffusing chemicals, change size or express different chemicals on the surface. Using the model he has demonstrated axis formation, segmented patterns, generation of hierarchical structures, regeneration after damage, axonogenesis, spiral growth and formation of cell layers [31, 32].

In real tissues cells are closely packed and tend to take on polyhedral shapes. This can be modeled through a topological representation where the cells are

vertices of a graph and neighboring cells linked by edges. The dual of the graph corresponds to the actual cells. This makes it easy to calculate neighbors and perform local chemical diffusion, and cell movement, cell division and cell death can be modeled by graph rewriting [33]. This was originally proposed by Matela and Fletterick [34] as a model of cell sorting.

Cell sorting occurs when different cell types are mixed with each other. The fragment of tissue rounds up into an almost spherical shape and one cell type aggregates centrally and another type surrounding it. If several types are included, they tend to form concentric shells. Steinberg suggested that cells adhere to each other with different strengths and interact to maximize adhesive energy [35]. This behavior can be modeled by allowing cells to attempt to move randomly, and if this move increases adhesion it will occur [36].

Another popular subject of multi-cell simulations is the behavior of slime molds. Slime molds begin their life as single-celled organisms that forage independently. When food becomes scarce they begin to aggregate, guided by a cyclic cAMP chemical signal secreted by groups of cells. They form a slug-like mass, which then differentiates into a tower-like spore capsule. Among other models, the Cell Programming Language of Pankaj Agarwal, which implements a topological representation, has been used to model the aggregation phenomenon [36]. A.F.M. Mare and P. Hogeweg have modeled the differentiation stage through a model including both cell adhesion, cAMP diffusion, pressure interaction and cell differentiation [37].

The use of topological models to model cell cleavage in the frog egg and neural differentiation in the fruit fly visual system has also been demonstrated [33]. In the later case a reaction-diffusion system was imposed on the cell graph and allowed to control the differentiation of the cells.

7 Phenomenological models

In addition to these attempts at biological realistic models of the emergence of differentiated organic structures, there are many approaches that are phenomenological. Phenomenological models do not try to model the underlying biological reality of the system strongly, but instead seeks to reproduce observed phenomena using simple models. See [38] for a brief tour.

Some of the most popular models are:

- Probabilistic models: growth is modeled as a stochastic process. A common application is describing the branching behavior of neurons, fitting the shapes to observed neuron properties (see [39, chapter 7] for a review).

- Cellular automata: a regular 1, 2 or 3-dimensional grid of cells is used, where each cell can have one of a discrete number of states. Each time-step all cells update their states according to a rule dependent only on their own state and the states of their neighbor. CAs are capable of exhibiting self-replicating behavior, reaction-diffusion dynamics, various growth and branching phenomena depending on the update rules.

- Diffusion-limited aggregation: growth occurs when diffusing particles connect to the growing structure, or proportional to the local concentration of a diffusing substrate depleted by the growth. This usually leads to a dendritic pattern. DLA has mainly been used for simulations in physics and inorganic chemistry, but also for modeling sponges [40].

- L-systems (Lindenmeyer systems): The organism is modeled as a string subjected to iterative rewriting corresponding to development, and the finished string is interpreted as a graphical object. Mainly used for plant modeling, although they have been used for cellular structures. Using context sensitive rules diffusion of plant hormones can be modeled. [41, 42]. The L-Neuron system of Ascoli and Krichmar uses a L-system to describe neuron topology and sizes, and then samples parameter values from experimental statistical distributions to generate multiple, non-identical virtual neurons [43, 44].

References

[1] J. Craig Venter, ..., and Xiaohong Zhu. The sequence of the human genome. *Science*, 291(5507):1304–1351, 2001.

[2] Alan Turing. The chemical basis of morphogenesis. *Phil. Trans. Roy. Soc. London*, B327:37–72, 1952.

[3] E. Atlee Jackson. *Perspectives of Nonlinear Dynamics*, volume 2. Cambridge University Press, 1990.

[4] Robin Engelhardt. *Modelling Pattern formation in Reaction-Diffusion Systems*. PhD thesis, University of Copenhagen, 1994. http://www.nbi.dk/~engelhar/spec/the.html.

[5] Igor S. Aranson and Lorenz Kramer. The world of the complex ginzburg-landau equation. *Reviews of Modern Physics*, 74(99), 2002.

[6] I. Farkas, D. Helbing, and T. Vicsek. Mexican waves in an excitable medium. *Nature*, 419:131–132, 2002.

[7] Hans Meinhardt. *Models of Biological Pattern Formation*. Academic Press, 1982.

[8] Hans Meinhardt. Biological pattern formation: How cell talk with each other to achieve reproducible pattern formation. http://www.rrz.uni-hamburg.de/biologie/b_online/e28_1/pattern.htm, 1999.

[9] Shugo Hamahashi and Hiroaki Kitano. Simulation of drosophilia embryogenesis. In *Proceedings of the 6th International Conference on Artificial Life (ALIFE-98)*, pages 151–160, Los Angeles, USA, 1998.

[10] Shugo Hamahashi and Hiroaki Kitano. Parameter optimization in hierarchical structures. In *Proceedings of the 5th European Conference on Artificial Life (ECAL)*, pages 467–471, Lausanne, Switzerland, 1999.

[11] Hans Meinhardt. *The Algorithmic Beauty of Sea Shells*. Springer, 1995.

[12] Roy Williams. Xmorphia. http://www.cacr.caltech.edu/ismap/image.html.

[13] R.A. Barrio, C. Varea, J.L. Aragon, and P.K. Maini. A two-dimensional numerical study of spatial pattern formation in interacting turing systems. *Bulletin of Mathematical Biology*, 61:483–505, 1999.

[14] Yannis Almirantis and Spyros Papageorgiou. Modes of morphogen cooperation for limb formation in vertebrates and insects. *J. theor. Biol*, 199:235–242, 1999.

[15] Hiroto Shoji, Yoh Iwasa, Atushi Mochizuki, and Shigeru Kondo. Directionality of stripes formed by anisotropic reaction-diffusion models. *Journal of Theoretical Biology*, 214:549–561, 2002.

[16] Philip Ball. *The Self-Made Tapstry: Pattern formation in nature*. Oxford University Press, 1999.

[17] C. Varea, J.L. Aragon, and R.A. Barrui. Turing patterns on a sphere. *Physical Review E*, 60(4):4588–4592, 1999.

[18] J.D. Murray. A pre-pattern formation mechanism for animal coat marking. *Journal of Theoretical Biology*, 88:161–199, 1981.

[19] S. Kondo and R. Asai. A reaction-diffusion wave on the skin of the marine angelfish *pomacanthus*. *Nature*, 376:765, 1995.

[20] J.D. Murray. How the leopard gets its spots. *Scientific American*, 259:80–87, 1988.

[21] J.D. Murray. *Mathematical Biology*. Springer-Verlag, Berlin, 1989.

[22] Arjen van Ooyen. Activity-dependent neural network development. *Network*, 5:401–423, 1994. http://www.anc.ed.ac.uk/~arjen/papers/review_abstract.html.

[23] H.G.E. Hentschel and Alan Fine. Instabilities in cellular dendritic morphogenesis. *Physical Review Letters*, 73(26), 1994.

[24] T.A. Hely, A. van Ooyen, and D.J. Willshaw. A simulation of growth cone filopodia dynamics based on turing morphogenesis patterns. In Mike Holcombe and Ray Paton, editors, *Information Processing in Cells and Tissues*, pages 69–73. Plenum Press, 1998. http://www.santafe.edu/ timhely/filopodia.ps.gz.

[25] T.A. Hely. *Computational Models of Developing Neural Systems*. PhD thesis, Dept. of Cognitive Science, University of Edinburgh, 1999. http://www.santafe.edu/ timhely/thesis.ps.gz.

[26] T.A. Hely, B. Graham, and A. van Ooyen. A computational model of dendrite elongation and branching based on map2 phosphorylation. *Journal of Theoretical Biology*, 1999. http://www.santafe.edu/ timhely/dendriteBranching.ps.gz.

[27] G.J. Goodhill. Mathematical guidance for axons. *Trends in Neuroscience*, 21(6):226–231, 1998.

[28] D.B. Dusenbery. Performance of basic strategies for following gradients in two dimensions. *Journal of theoretical Biology*, 208:345–360, 2001.

[29] H.G.E. Hentschel and A. van Ooyen. Models of axon guidance and bundling during development. *Proc. R. Soc. Lond B*, 266:2231–2238, 1999. http://www.anc.ed.ac.uk/~arjen/papers/bundle_abstract.html.

[30] Hiroaki Kitano, Shugo Hamahashi, Jun Kitazawa abd Koji Takao, and Shin icirou Imai. The virtual biology laboratories: A new approach to computational biology. In *The 4th European Conference on Artificial Life (ECAL-97)*, Brighton, UK, 1997.

[31] Kurt W Fleischer and Alan H. Barr. A simulation testbed for the study of multicellular development: the multiple mechanisms of morphogenesis. In *Artificial Life III*, pages 389–408. Addison-Wesley, 1994. ftp://ftp.gg.caltech.edu/pub/Papers/kurt_alife94.ps.Z.

[32] Kurt W. Fleischer. *A Multiple-Mechanism Developmental Model for Defining Self-Organizing Geometric Structures*. PhD thesis, California Institute of Technology, 1995. http://waggle.gg.caltech.edu/~kurt/Devsim/devsim.html.

[33] Sharon Duvdevani-Bar and L. Segel. On topological simulations in developmental biology. *Journal of Theoretical Biology*, 131:33–42, 1988.

[34] Raymond J. Matela and Robert J. Fletterick. Computer simulation of cellular self-sorting: A topological exchange model. *Journal Of Theoretical Biology*, 84:673–690, 1980.

[35] Malcolm S. Steinberg. Does differential adhesion govern self-assembly processes in histogenesis? *JEZ*, 73:395–434, 1970.

[36] Pankaj Agarwal. The cell programming language. *Artificial Life*, 2(1):37–77, 1994.

[37] Athanasius F.M. Marée and Paulien Hogeweg. Modelling *dictyostelium discoideum* morphogenesis: the culmination. *Bulletin of Mathematical Biology*, 64:327–353, 2002.

[38] Przemyslaw Prusinkiewicz, Mark Hammel, and Radomir Mech. Visual models of morphogenesis: A guided tour. http://www.rrz.uni-hamburg.de/biologie/b_online/virtuallaboratory/TitlePage.html, 1997.

[39] Erik de Schutter, editor. *Computational Neuroscience: Realistic Modelling for Experimentalists.* CRC, 2001.

[40] J. Kaandorp. *Modeling growth forms of biological objects using fractals.* PhD thesis, University of Amsterdam, 1992.

[41] Przemyslaw Prusinkiewicz and Aristid Lindenmayer. *The Algorithmic Beauty of Plants.* Springer, 1990.

[42] Gabriela Ochoa. An introduction to lindenmayer systems. http://www.rrz.uni-hamburg.de/biologie/b_online/e28_3/lsys.html, 1998.

[43] Giorgio A. Ascoli and Jeffrey L. Krichmar. L-neuron: A modeling tool for the efficient generation and parsimonious description of dendritic morphology. *Neurocomputing*, 32–33:1003–1011, 2000.

[44] Giorgio A. Ascoli. Progress and perspectives in computational neuroanatomy. *Anatomical Record*, 257(6):195–207, 1999.